 Human Molecular Genetics, 1996, Vol. 5, No. 1 51–59

ARTICLE

An animal model for Norrie disease (ND): gene targeting of the mouse ND gene

Wolfgang Berger[1,2,*], Dorien van de Pol[1], Dietmar Bächner[3,+], Frank Oerlemans[4], Huub Winkens[5], Horst Hameister[3], Bé Wieringa[4], Wiljan Hendriks[4] and Hans-Hilger Ropers[1,2]

[1]Department of Human Genetics, University Hospital Nijmegen, Nijmegen, The Netherlands, [2]Max-Planck-Institut für Molekulare Genetik, Berlin, Germany, [3]Abteilung für Klinische Genetik, Universität Ulm, Ulm, Germany, [4]Department of Cell Biology and Histology, University Nijmegen, Nijmegen, The Netherlands and [5]Department of Ophthalmology, University Hospital Nijmegen, Nijmegen, The Netherlands

Received September 14, 1995; Revised and Accepted October 27, 1995 EMBL accession number: X92397

In order to elucidate the cellular and molecular processes which are involved in Norrie disease (ND), we have used gene targeting technology to generate ND mutant mice. The murine homologue of the ND gene was cloned and shown to encode a polypeptide that shares 94% of the amino acid sequence with its human counterpart. RNA *in situ* hybridization revealed expression in retina, brain and the olfactory bulb and epithelium of 2 week old mice. Hemizygous mice carrying a replacement mutation in exon 2 of the ND gene developed retrolental structures in the vitreous body and showed an overall disorganization of the retinal ganglion cell layer. The outer plexiform layer disappears occasionally, resulting in a juxtaposed inner and outer nuclear layer. At the same regions, the outer segments of the photoreceptor cell layer are no longer present. These ocular findings are consistent with observations in ND patients and the generated mouse line provides a faithful model for study of early pathogenic events in this severe X-linked recessive neurological disorder.

INTRODUCTION

Norrie disease (ND) is an X-linked recessive neurodegenerative condition with ocular atrophy as the most conspicuous sign. The disorder is characterized by congenital or early childhood blindness due to proliferative and degenerative changes in the vitreous body and the retina. First manifestations of ND are bilateral white retrolental membranes or masses, which are present at birth or appear during the first months of life. Histopathological examinations showed retinal detachment, falciform fold of the retina, and fibrovascular tissue present in the vitreous body (1,2). In early stages, the differential diagnosis of ND includes retinoblastoma, Coat's disease, juvenile retinoschisis, autosomal recessive falciform detachment, persistent hyperplastic primary vitreous, retrolental fibroplasia, metastatic endophthalmitis and massive retinal fibrosis (3). In later stages, the eyes begin to shrink and become atrophic. Extraocular features of ND are sensorineural deafness and mental disturbances, often with psychotic features, occurring in at least one-third of the cases. Moreover, atypical patients have been reported, with hypogonadism, microcephalus, growth retardation, immunodeficiency and epileptic seizures as additional symptoms (4–9). As in several of these patients DNA deletions encompassing the DXS7 locus at Xp11.4 had been detected, a contiguous gene syndrome has been suggested to explain these complex phenotypes (7–11). Subsequently, smaller deletions were found, and their molecular characterization paved the way for the isolation of a candidate gene for ND by positional cloning (12–14). Deletions occur in approximately 20% of the patients and vary in size from 2 to several hundred kbp.

Numerous point mutations have been detected, which lead to truncated or elongated gene products, but more frequently to amino acid substitutions (15–18). These studies also revealed that not only the ocular symptoms, but also mental disturbances and deafness are pleiotropic effects of a single mutation (15) and that a less severe condition, X-linked familial exudative vitreoretinopathy, is allelic to ND (19). The genomic size of the ND gene is 28 kbp and it consists of three exons with a total transcript length

*To whom correspondence should be addressed at: Max-Planck-Institut für Molekulare Genetik, Ihnestrasse 73, D-14195 Berlin (Dahlem), Germany

+Present address: Department of Molecular Biology, GBF, Braunschweig, Germany

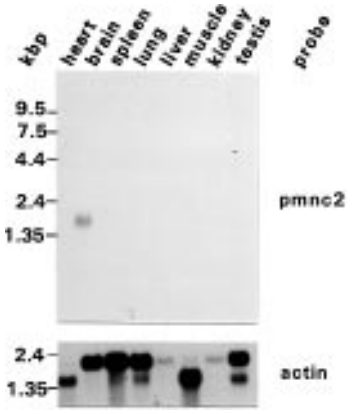

Figure 1. Hybridization of a multiple tissue Northern blot containing poly(A)$^+$-RNA of indicated adult mouse organs and tissues using the mouse ND gene cDNA pmnc2 as a probe. In the lower panel, hybridization with an actin cDNA control probe is shown. Each lane contains 2 µg RNA.

of 1.9 kbp. The open reading frame (ORF) of 399 bp is completely contained within exons 2 and 3 and gene expression is restricted to brain and retina as revealed by Northern blot analysis.

The predicted gene product contains 133 amino acid residues, is probably secreted and particularly rich in cysteines. Database searches revealed homologies of the ND protein with the cysteine-rich domain of mucins and with proteins involved in cell interaction and differentiation processes (20). Moreover, computer modelling of the tertiary structure of the ND gene product revealed striking similarities with the transforming growth factor β (TGFβ) (21). These observations point to a role of the ND gene product in developmental and differentiation processes. However, little is known about the histological, cellular and molecular mechanisms which are involved in the pathogenesis of this disease. To shed more light on the sequence of events involved in the manifestation of ND, we have established an animal model for this disorder by targeted mutagenesis of the Norrie disease (mND) gene of the mouse.

RESULTS

The mouse Norrie disease (mND) gene and its expression pattern

A human complementary DNA clone, pTF35 (12), which spans the entire ORF and parts of the 5′ and 3′ noncoding regions, was used as probe to screen a mouse brain cDNA library. Isolated cDNAs detected a 1.8 kbp transcript in mouse brain by Northern blot hybridization (Fig. 1). X-chromosomal localization was established by dosage Southern blot hybridization (data not shown) and confirmed later on by hybridization of gene targeted XY embryonic stem cell lines with the deleted 283 bp exon 2 fragment (Fig. 4b). There is a high degree of nucleotide sequence conservation between the human and mouse ND gene. Sequence comparison yielded identity values of 91.7% for the ORF and 82.3% for the entire cDNA. The exon–intron structure of the mND gene was established by cloning the cDNA hybridizing genomic *Eco*RI fragments from mouse strain 129/SvJ DNA and subsequent sequencing of intron–exon junctions with cDNA-derived primers. The gene consists of three exons hybridizing to *Eco*RI fragments of 2.5, 6.5 and 4.0 kbp, respectively, and

```
   1 ACACTCTCCC TCTCTCTCTC CCTCTCTCTC CCTCTCTCTC TCTCCCTCTC   50
  51 TCTCCCTCTC TCTCCCTGGG TCGCTTAAAC AACAGTCCTA ACTTTTGTGT  100
 101 GTTGCAAATA TAAAAGCAAG CCATGTGACA GAGGGACAGA AGAACAAAAG  150
 151 CATTTGGAAG TAACAGGTCC TCTTTCTAGC TCTCAGAAAA GTCTGAGAAG  200
 201 AAAGGAGCCC TGCGTTTCCC CCAAG              intron 1
          intron 1              CTGTG CAGCACATAC TGCTGTGATC  250
 251 GGTTGCAAGT GAAAGAAGCA AGAGAAATTC CTGATTCCCA AAGGACAATG  300
 301 ACAACCAGAA AGCGGCAGCC CTATCCTGCT CTGGCCTTGA AAGGACTGGA  350
 351 TCCTAGGAGG TGGCAGCATT TCCAATCTAT TGTCCTCTGT CTCCCTCTGC  400
 401 TGTTTTTCTG GAGGAGTTTC CCTTTACAAC AATGAGAAAT CATGTACTAG  450
 m                                   M  R  N   H  V  L  A
 h                                            K
 451 CTGCATCCAT TTCTATGCTC TCCCTGCTGG CCATAATGGG AGATACAGAC  500
 m    A  S  I   S  M  L   S  L  L  A   I  M  G   D  T  D
 h       F                    V
 501 AGCAAAACAG ACAGTTCATT TCTGATGGAC TCTCAACGCT GCATGAGACA  550
 m  S  K  T  D   S  S  F   L  M  D   S  Q  R  C   M  R  H
 h                          I           D
 551 CCATTATGTC GATTCTATCA GTCACCCACT GTACAAATGT AGCTCAAAG   559
 m   H  Y  V   D  S  I  S   H  P  L   Y  K  C   S  S  K
 h
          intron 2                                        A  600
 m                                                        M
 h
 601 TGGTGCTCCT GGCCAGATGT GAGGGGCACT GCAGCCAGGC ATCACGCTCT  650
 m    V  L  L   A  R  C   E  G  H  C   S  Q  A   S  R  S
 h
 651 GAGCCCTTGG TGTCCTTCAG CACTGTCCTC AAGCAACCTT TCCGTTCCTC  700
 m  E  P  L  V   S  F  S   T  V  L   K  Q  P  F   R  S  S
 h
 701 CTGTCACTGC TGCCGACCCC AGACTTCCAA GCTGAAGGCT CTGCGTCTGC  750
 m   C  H  C   C  R  P  Q   T  S  K   L  K  A   L  R  L  R
 h                                                        -
 751 GCTGCTCAGG GGGCATGCGA CTTACTGCCA CTTACCGGTA CATCCTCTCC  800
 m    C  S  G   G  M  R   L  T  A  T   Y  R  Y   I  L  S
 h
 801 TGTCACTGTG AGGAATGCAG CTCCTGAGAC TTACTAGTGA TTGGCTTTCT  850
 m  C  H  C  E   E  C  S   S  *
 h              N
 851 GACTGGCACG GCCACAGGAG CAGTTCAACC TGCCAGAGAC GGACTGGCAA  900
 901 GAAAAGAGTT AAGGCAGATA AAGATGGAGC AAGTCCCATA GGATTTTGCA  950
 951 TATTCTTGTC CTAAAGACTC AATGTGCTTT TGACAGAAAG TGACTCTGGG 1000
1001 AACTTGCTTT TCATTCCCAT CTCCTTTCCC TGGAAGAATT TCTTTTGGTT 1050
1051 ACTTTACAGA TTCAGGCATT TCCCCTGTTG GCTCTAATTG TGGTTTGGGT 1100
1101 GCCTGACAGT CTCGCATTAG TGGGAAAATG TGGGGCCCGG GGCAATAGCA 1150
1151 TGTCAGGCTG TTCCTATTTG GTGCATATTA GGGAAAATTT TACCTAACCC 1200
1201 TCCTTAGGAG ATCTTTGCCT TGTTGTTTCC CCTGGTCATT TGGTCTAAGA 1250
1251 TTTGCCTCTA AAGTTTCCTG GTTTCAGATC TGGACACCCA GTCCATGGAT 1300
1301 GTTTAGTGAG GCTTACTCAC AGCCAGCTAA CTGCTACTAA AATAACTAAC 1350
1351 ACATGGGTTC TTTTATGTGA CAGCGGGACT CCTGACCACT ATAGTAATTA 1400
1401 TTCAGAAGTG ACTGAGGGGA TATAAATGTG GCAGAGGAAT TTATAATCTG 1450
1451 AAGCCTTTTG TGAGGAAGCA GGCTTTCACA CATACACACT CAGGTGGATC 1500
1501 CTGCACTGAC TCTGGAGAAG GCATACATTA TACTTGGTGT GGAGAACACA 1550
1551 CCATACTCAT AATTGAGCAT TAGTCAAGCA TGTAGGAATC TACTTGTGGG 1600
1601 TGTGCAATAG CTTCAGCCAT ATCTTAGCTA TATCCACCTG TCTATGTGAA 1650
1651 GCTTGTTGCC GTAGTGGTGG CCCGACTTAT TGTCTGAAAT TTTTGTTTCA 1700
1701 ATATATTTTT GGTCCTCGAA GCTCAAATTT TGAAGTCTCC CCATGTTTTC 1750
1751 AAATAAAAAT AAGAAGTAAC CTTC(AA)n
```

Figure 2. Nucleotide sequence of the mouse cDNA clone pmnc2. The interruption of the cDNA sequence by two introns has been determined by sequencing corresponding genomic clones. The startcodon at positions 432–434 and the polyadenylation signal at positions 1752–1757 are underlined. The mouse (m) amino acid sequence and residues which differ in the human (h) polypeptide are given in single letter code.

encodes a polypeptide of 131 amino acids. The human and mouse protein sequences are 94% identical, with only minor substitutions (Fig. 2).

In order to investigate tissue specific expression of the mND gene, RNA *in situ* hybridization was carried out. Expression was low and evenly distributed in almost all tissues of mouse embryos from 12.5 to 18.5 days post conception (d.p.c.), including the eye, ear and brain. Enhanced expression was visible in the developing olfactory bulb at 14.5 d.p.c. (data not shown). Here, high expression is restricted to differentiating neurons of the marginal layer. Two weeks after birth, the expression within the olfactory bulb becomes restricted to the mitral cell layer and the sensory layer of the olfactory epithelia (Fig. 3g–k). High expression levels

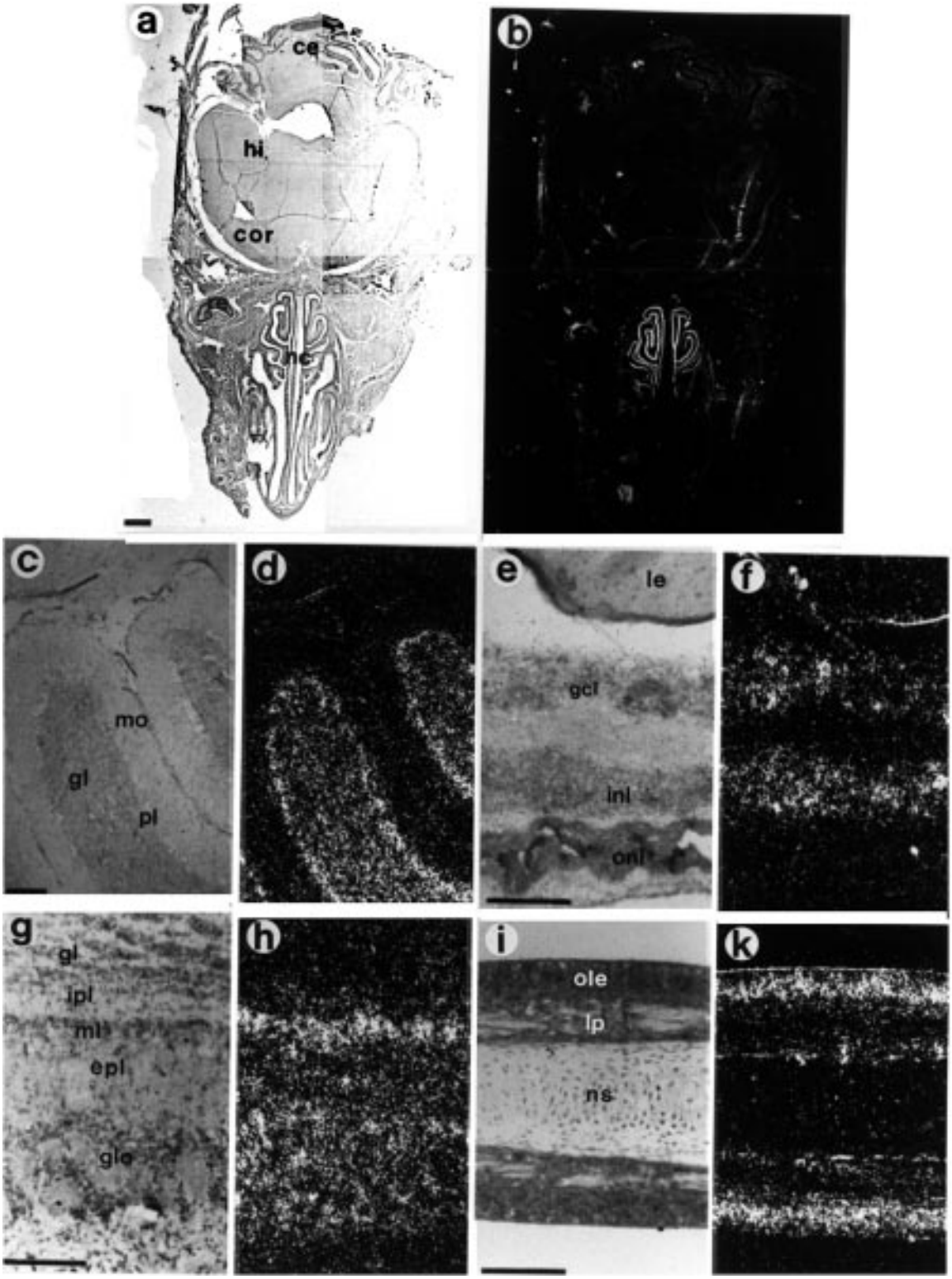

Figure 3. RNA *in situ* hybridization of a mND gene riboprobe to a transversal cryosection of a mouse head 2 weeks after birth. Bright field (**a, c, e, g** and **i**) and corresponding dark field (**b, d, f, h** and **k**) images are shown. High expression is visible in the olfactory epithelium and the retina and lower expression levels were detected in the cerebellum (b). The high magnifications of the different tissues show expression within the Purkinje cell layer of the cerebellum (c and d), the retinal ganglion and inner nuclear layers (e and f), the mitral cells of the bulbus olfactorius (g and h) and in the olfactory epithelium (i and k). ce: cerebellum, cor: cortex, epl: external plexiform layer, gcl: ganglion cell layer, gl: granular layer, glo: glomerular layer, hi: hippocampus, inl: inner nuclear layer, ipl: internal plexiform layer, le: lens, lp: lamina propria, ml: mitral cell layer, mo: molecular layer, nc: nasal cavity, ns: nasal septum, ole: olfactory epithelium, pl: Purkinje cell layer. Bars a and b: 1 mm; c-k: 100 μm.

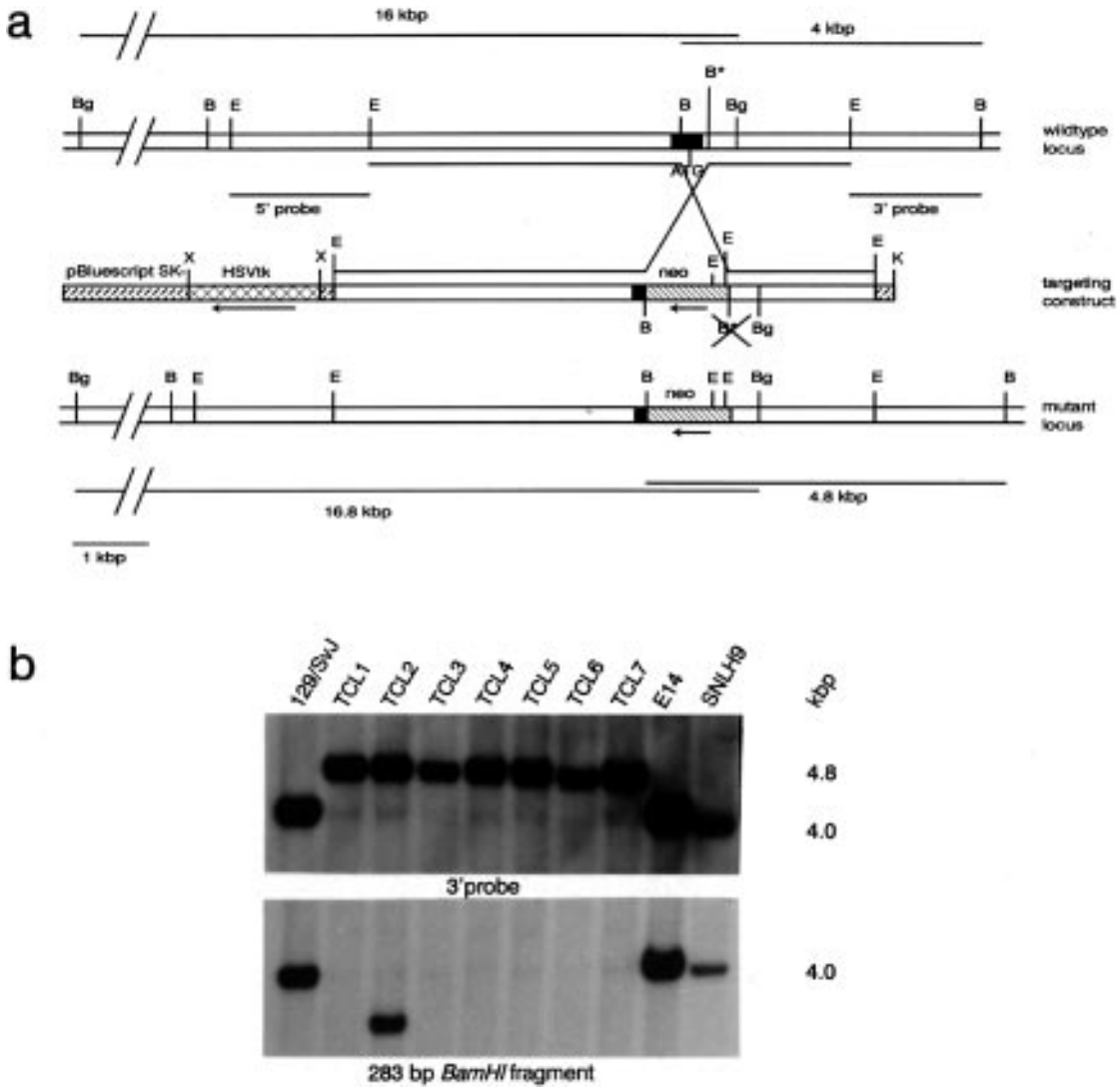

Figure 4. Gene targeting of the murine ND gene. (**a**) Targeting strategy. A portion of exon 2 (black box) was replaced by a neomycin resistance cassette (neo, shaded box). The targeting vector contained the thymidine kinase gene of the herpes simplex virus (hsvtk) as additional selection marker. Correctly targeted clones will show a 4.8 kbp *Bam*HI and a 16.8 kbp *Bgl*II fragment with the 3′ and 5′ probes, respectively. Both of these probes are located external to the targeted 6.5 kbp *Eco*RI fragment. Restriction sites: B, *Bam*HI; B*, *Bam*HI introduced by *in vitro* mutagenesis; Bg, *Bgl*II; E, *Eco*RI; K, *Kpn*I; X, *Xba*I. (**b**) Autoradiogram of a Southern blot containing *Bam*HI digested DNA of seven targeted embryonic stem cell lines (TCL) and controls (129/SvJ: liver DNA from mouse strain 129/SvJ, E14: DNA of non targeted embryonic stem cells, SNLH9: DNA isolated from feeder cells) after hybridization with the 3′ probe (top) and the substituted 283 bp fragment from exon 2 (bottom).

were also observed in the inner nuclear layer as well as the ganglion cell layer of the retina (Fig. 3e,f) and in Purkinje cells of the cerebellum of 2 week old mice (Fig. 3c,d). We were not able to detect any specific expression in the ear in animals at the age of 4 weeks. Moreover, there was no significant expression in gonads, kidney, liver, lung, spleen, gut, and tongue of adult animals (4–6 months).

Gene targeting of murine embryonic stem (ES) cells

To replace the wild-type ND gene by an inactive gene copy in mouse embryonic stem cells, we designed a construct carrying a deletion of the protein coding portion of exon 2, which removes the 56 N-terminal amino acids of the ND gene product as shown in Figure 4a. Prior to gene targeting in ES cells from mouse strain 129, a genomic 6.5 kbp *Eco*RI fragment carrying exon 2 of that strain was preparatively cloned, because it had been shown previously that isogenic gene targeting constructs yield the highest efficiencies (22). Subsequently, this *Eco*RI fragment was recloned in a *Bam*HI deficient pBluescript SK$^-$ vector and a second *Bam*HI site was introduced behind the boundary between exon 2 and intron 2 by *in vitro* mutagenesis. This and the *Bam*HI site 5′ to the ATG start codon, were used to replace 283 bp of exon 2 by a neomycin resistance cassette, in the opposite transcriptional orientation. Additionally, the HSVtk gene was introduced in front of the 5′ end of the homologous *Eco*RI fragment, again in opposite orientation to the mND gene (Fig. 4a), to allow for negative selection against random integration events with FIAU.

After electroporation of this construct and selection with G418, 192 resistant clones were obtained, seven of which gave the expected diagnostic 4.8 kbp *Bam*HI fragment after hybridization with a 3′ probe (Fig. 4a,b). With a 5′ probe, six of these clones

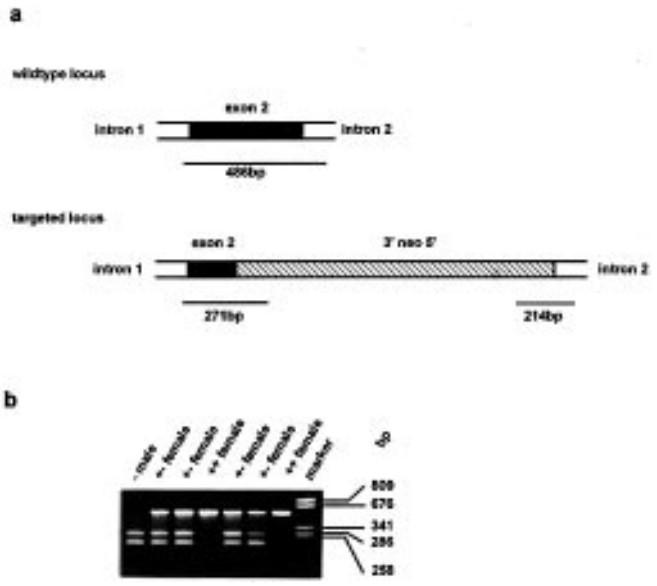

Figure 5. PCR-genotyping of mouse tail DNA. (**a**) Genotyping strategy. Amplification of the endogenous wild-type locus with two intron primers results in a fragment of 486 bp, while from the targeted locus two fragments of 271 and 214 bp are being amplified by using combinations of intron primers and neo-cassette primers. (**b**) Ethidium bromide stained agarose gel of PCR fragments derived from hemizygous mutant mice (–), as well as heterozygous (+–) and homozygous (++) females.

showed also the diagnostic 16.8 kbp *Bgl*II fragment indicative for a faithful homologous recombination upstream of exon 2. The loss of the coding segment of exon 2 was confirmed by using the replaced fragment as probe (Fig. 4b). All properly targeted cell lines were karyotyped prior to injection. Five cell lines containing the normal number of 40 acrocentric chromosomes were injected into C57Bl/6 blastocysts and embryos were transferred to pseudopregnant carrier mothers. One of the cell lines gave rise to chimeric male offspring that transmitted the mutation through the germ line. F_1 heterozygous females were mated with wild-type (wt) males and the offspring (F_2) was genotyped by PCR with primer combinations allowing the identification of the wild type as well as the mutant allele in a single assay (Fig. 5a,b).

Analysis of ND mice

In the F_1 offspring of heterozygous females, the four expected genotypes were almost equally represented, with a small preponderance of heterozygous females. Among 267 F1 animals, 135 were female; of these, 78 were heterozygous ($\chi^2 = 3.267$, $P = 0.089$). A total of 65 hemizygous mutant mice were identified by PCR on DNA from tail tips removed 14 days after birth.

Initial ophthalmological examinations were performed with a slit-lamp, 3 weeks after birth. In three of six hemizygous mutant mice examined, conspicuous precipitate-like retrolental structures were seen in the vitreous body. Slit-lamp examination of older mutant mice (10–20 weeks) revealed pathological signs in nine of nine cases. These differences point to a variable age of onset. In contrast, the variation in number and size of the precipitates was age independent. The control group, consisting of 10 wt animals, was found to be completely normal upon slit-lamp examination. Apart from these precipitate-like structures, depigmented bundles or stripes were present in some of the eyes of hemizygous mutant mice, which were interpreted as retinal folding or detachment.

Table 1. Ophthalmologic examination of hemizygous mutant mice by slit-lamp biomicroscopy and morphohistological analysis

Mouse ID#	Age (weeks)	Eye	Slit-lamp	os	onl	inl	gcl	vb
5	10	L	+	+	+	+	+	+
		R	+	+	+	+	+	+
9	26	L	+	+	+	+	+	+
		R	+	+	+	+	+	+
32	4	L	+	–	–	+	+	+
		R	+	–	+	+	+	+
112	22	L	+	–	–	+	+	+
		R	+	–	–	+	+	+
244	18	L	+	+	+	+	+	+
		R	+	+	+	+	+	+
270	12	L	+	+	+	+	+	+
		R	+	–	–	+	+	+
304	10	L	+	+	+	+	+	+
		R	+	+	+	+	+	+
322	8	L	+	–	–	+	+	+
		R	+	–	–	+	+	+
348	6	L	+	+	+	+	+	+
		R	+	–	–	–	+	+

From each mouse the left (L) and the right (R) eye were examined. Pathological changes within the outer segments (os) of the photorecepor layer, the outer and inner nuclear layer (onl, inl), the ganglion cell layer (gcl), and the vitreous body (vb) are indicated by +. Morphological analysis was performed on sections of 5 μm, obtained every 100 μm.

First morphohistological data were obtained from enucleated eyes of nine hemizygous mutant mice aged between 4 and 26 weeks (Table 1). The most prominent findings in histological sections were fibrous masses within the vitreous bodies of all eyes examined. The nature and origin of these retrolental patterns are unclear. They are probably the histological equivalent of the precipitate like structures, seen upon slit-lamp examination. Another conspicuous finding in the retinae of hemizygous mutant mice was an overall disorganization of the ganglion cell layer. In the normal retina of control mice, the nuclei of the ganglion cell layer are arranged in a 'string of pearls'-like fashion (Fig. 6a). In contrast, nuclei in the ganglion cell layer of the retinae of mutant mice showed an overall disorganized appearance and some of them seem to migrate into the inner plexiform layer (Fig. 6b–f). Whereas the ganglion cell layer of mutant mice is completely affected, changes within the inner and outer nuclear layers as well as the outer segments of the photoreceptor layer occur occasionally. Beside severely affected regions, the major part of these layers is morphologically inconspicuous. Within the severely affected areas, the outer plexiform layer and the outer segments of the photoreceptor cells disappear and hyperpigmentation of the retinal pigment epithelium became evident (Fig. 6c,f). At some of these sites, nuclei from the outer nuclear layer are displaced into the outer plexiform and the inner nuclear layer (Fig. 6b,c), and also the opposite, a relocation of nuclei from the inner nuclear into the photoreceptor layer has been found. The latter culminates in the disappearance of the photoreceptors (Fig. 6f). A rather mild phenotype with respect to the inner nuclear and the photoreceptor layers has been observed in all sections of a 22 week old hemizygous mutant mouse. The photoreceptor layer of this animal, although slightly undulated, is inconspicuous at the morphological level and only the inner nuclear layer showed a mild degree of disorganization (Fig. 6e). However, the ganglion cell layer is affected in a characteristic manner and retrolental structures were present within the vitreous body. Thus, even when inner nuclear and photoreceptor layers are only mildly affected, the changes within the vitreous body and the ganglion cell layer are prominent. These findings may serve as an indication for the primary nature of these pathogenic events in murine ND.

In addition to the analyses in hemizygous mutant mice we have examined three heterozygous females at the age of 3, 8 and 12 weeks, respectively. Slit-lamp biomicroscopy revealed no changes within the vitreous body. Morphohistological analysis of the retina from the 8 week old carrier female showed a normally developed retina.

DISCUSSION

Retrolental masses, falciform fold of the retina and retinal detachment are the most common and prominent ocular findings in ND patients. Very little is known about the early histological manifestations of the disease which precede these changes as most of the available histological data were obtained from eyes enucleated because of suspected retinoblastoma, that is, from patients with an advanced stage of the disease. By cloning the murine homologue of the human ND gene and its targeted inactivation in embryonic stem cells, we have established a mouse model for ND. Upon slit-lamp biomicroscopy of hemizygous mutant mice, changes within the vitreous body were observed that were strikingly similar to early ocular manifestations of ND in humans. Subsequently, morphological studies were performed to obtain insight in the cellular events preceding overt clinical signs of the disease.

There are two different hypotheses regarding the primary defect and early manifestations in ND. On the one hand, a neuroectodermal defect has been assumed that induces an early arrest in retinal development with associated malformation in related development of the primary and secondary vitreous (23). On the other hand, it has been assumed that proliferative changes resulting in the formation of retrolental membranes and masses represent the initial step, and that retinal abnormalities are secondary (24). According to this hypothesis, degeneration of the retina is a result of tractional forces, leading to a reduction of the trophic function of the RPE due to dissociation of the latter from the developing retina.

In mice with targeted inactivation of the ND gene, histological data suggest retrolental structures and a disorganized ganglion cell layer as primary pathogenic events. Changes within the adjacent retinal layers, i.e. the inner nuclear and the photoreceptor layer, occur occasionally and are therefore probably secondary. Thus, at least in mice, the differentiation of the retina seems to be normal initially.

According to our findings, the ND gene product could play a crucial part in the onset of late differentiation processes in the retina or, more likely, in the fixation of differentiated states, either by establishing cell–cell contact or programming particular expression patterns via intracellular signalling mechanisms. The similarity of the tertiary structure between the ND gene product and the transforming growth factor β (TGFβ), predicted by computer modelling of the human ND polypeptide (21), may justify its affiliation to a structural superfamily of growth factors containing a cysteine knot motif (25). These factors are known to be involved in the regulation of differentiation processes, and in particular TGFβ has the potential to influence intracellular signalling but also transcriptional regulation of genes involved in extracellular matrix turnover (26,27).

MATERIALS AND METHODS

Isolation of mND gene sequences

One million p.f.u. of a mouse brain cDNA library (Stratagene, #937301) were plated on *Escherichia coli* XL-Blue cells at a density of 50 000 per 15 cm Petri dish. Replicas were made on nitrocellulose membranes and filters were screened with the human ND gene cDNA clone pTF35 (12) at 55°C in 6×SSC, 10% dextransulphate, 5×Denhardt's, 0.2% SDS and 100 µg/ml herring sperm DNA. Washing was carried out in 2×SSC, 0.2% SDS and finally 0.1×SSC, 0.2%SDS at 55°C. Positive clones were sequenced using the Pharmacia T7 sequencing kit with ^{35}S-dATP labelling. The murine consensus cDNA and the predicted

Figure 6. Morphological analysis of 5 µm sections from paraffin embedded eyes of control (a) and hemizygous mutant (b–f) mice. (**a**) Section through the eye of a 10 week old wild-type male offspring from a heterozygous female. Morphological analysis of eyes from gene targeted males was performed at the age of 6 (**b**), 10 (**c**), 12 (**d**), 22 (**e**) and 26 (**f**) weeks after birth. The 5 µm sections were stained with hematoxylin and eosin. Magnification: ×180. c, choroid; gcl, ganglion cell layer; inl, inner nuclear layer; onl, outer nuclear layer; os, outer segments of the photoreceptor cells; rpe, retinal pigment epithelium; vb, vitreous body.

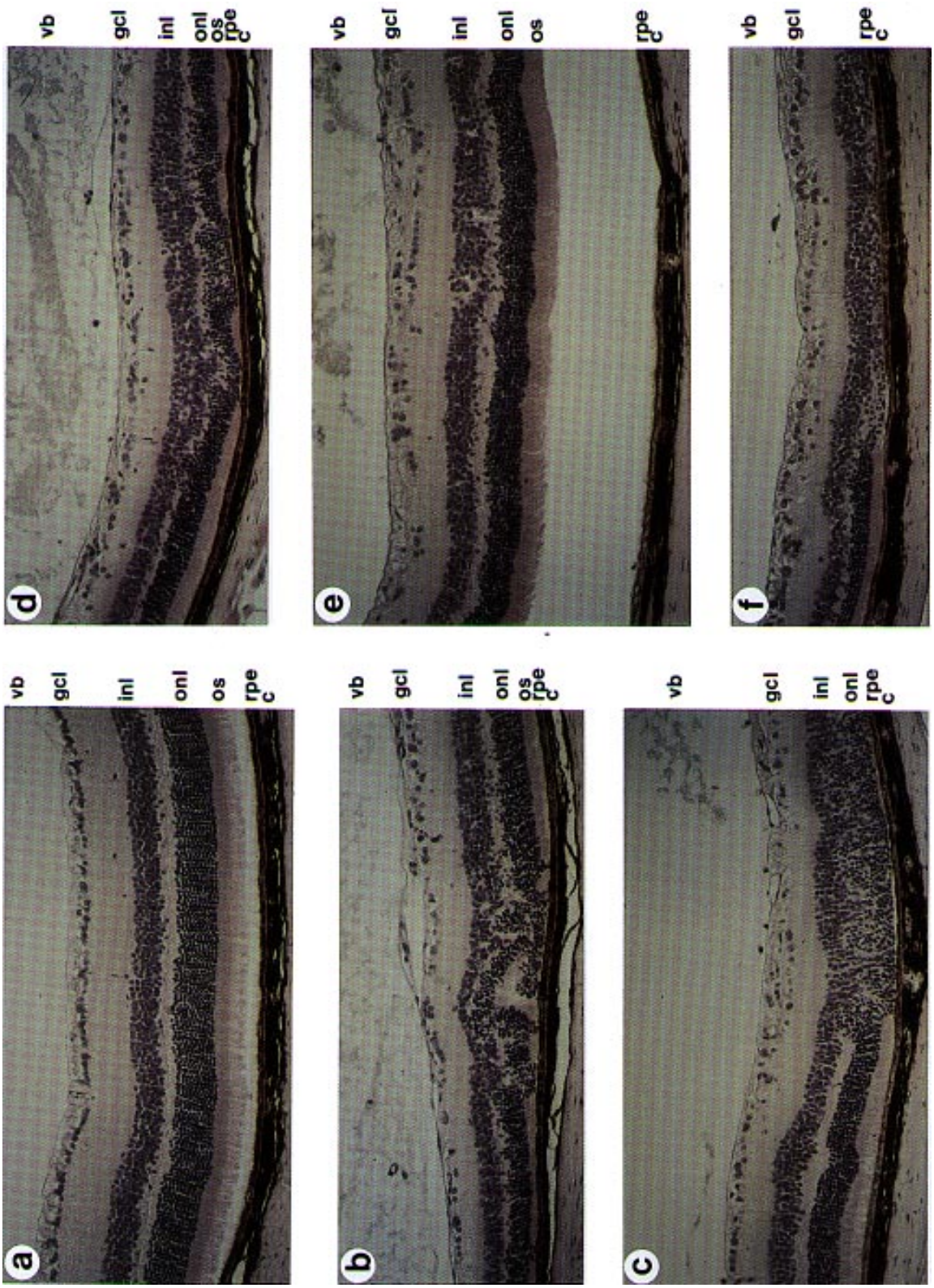
a
vb
gcl
inl
onl
os
rpe
c
b
vb
gcl
inl
onl
os
rpe
c
c
vb
gcl
inl
onl
rpe
c
d
vb
gcl
inl
onl
os
rpe
c
e
vb
gcl
inl
onl
os
rpe
c
f
vb
gcl
rpe
c

polypeptide sequences were used for database screening (EMBL as well as SwissPir).

Genomic fragments of the mND gene were cloned preparatively from *Eco*RI or *Bam*HI digested liver DNA from mouse strain 129/SvJ. Restriction fragments were separated in a preparative 0.8% low melting temperature agarose gel at 40 V in 40 mM Tris-acetate pH 7.5 and 1 mM Na_2 EDTA for 16 h. The gel was sliced into 2 mm fractions, aliquots of 75 µl each were incubated at 65°C and dot-blotted on GeneScreenPlus membrane, hybridized with pmnc2 and the DNA of positive fractions was purified by making use of the GeneClean protocol (Bio101). The fragments were cloned into λZAP and λZAPEXPRESS for *Eco*RI and *Bam*HI fragments, respectively. The exon containing *Eco*RI fragments of 2.5 (exon1), 6.5 kbp (exon2) and 4 kbp (exon3) were used to establish the intron–exon boundaries of the mND gene by sequencing with cDNA-derived primers.

The two preparatively isolated *Bam*HI fragments of 6.5 and 4 kbp were used for the isolation of the 5′ and 3′ probes, respectively, which are represented by a 1.8 kbp *Eco*RI and a 1.7 kbp *Eco*RI–*Bam*HI fragment and situated external with respect to the targeted 6.5 kbp *Eco*RI fragment.

Expression studies

Northern blots containing poly(A)$^+$ RNA from adult tissues (Clontech) were hybridized with the mouse cDNA pmnc2 according to the manufacturers instructions. Northern blots of fetal RNA samples were made by separating 10–20 µg total RNA from different tissues, isolated by the guanidinum isothiocyanate method (28), in a 1% agarose gel containing 8% formamide and subsequent blotting on to GeneScreenPlus membranes. Hybridization was performed according to standard methods (29).

For RNA *in situ* hybridization whole embryos or single organs of mice were fixed overnight with 4% paraformaldehyde in PBS at 4°C and prepared for cryostat sections and *in situ* hybridization was carried out as described (30). Briefly, antisense and sense probes were generated by *in vitro* transcription with α^{35}S-dUTP using the *Eco*RI and *Xho*I linearized plasmid pmnc2 and the T7 or T3 RNA polymerase, respectively. The probe length was reduced to 150–200 nucleotides by alkaline hydrolysis. The slides containing tissue sections were prehybridized at 54°C in a solution containing 50% formamide, 10% dextrane sulfate, 0.3 M NaCl, 10 mM Tris, 10 mM sodium phosphate pH 6.8, 20 mM DTT, 0.2×Denhardt's, 0.1% Triton-X-100, 0.1 mg/ml *E.coli* RNA, and 0.1 mM αS-UTP. For hybridization, 80 000 d.p.m./µl labelled RNA probe was added to the hybridization mix, incubated for 16 h at 54°C in a humid chamber, and washed in hybridization solution. After RNase A digestion the slides were washed 30 min 37°C in 2×SSC; 0.1% SDS, 30 min in 0.1×SSC and dehydrated by increasing concentrations of ethanol. The slides were coated with Ilford K5 photoemulsion for autoradiography. After 2–3 weeks of exposure at 4°C, developing was performed in Kodak D19b. Slides were subsequently stained with Giemsa and embedded. The sections were analysed with bright- and dark-field illumination using a Zeiss SV8 stereomicroscope and an Axiophot microscope.

Construction of the replacement vector

The 6.5 kbp genomic *Eco*RI fragment from mouse strain 129/SvJ, which contains exon 2 of the mND gene, was cloned into a *Bam*HI deficient pBluescript SK– vector. Additionally, to the natural present *Bam*HI site in front of the ATG start codon, a second *Bam*HI recognition sequence was introduced by *in vitro* mutagenesis employing the following primer: 5′ gggagaaggg-gatcctccaaa 3′ (Isogen Bioscience, The Netherlands). Briefly, uridine containing single stranded DNA was isolated by using the helper phage VCSM13 (Stratagene, #200251), annealed to the above mentioned 5′ phosphorylated oligonucleotide, and the second strand was synthesized with Klenow DNA polymerase. After ligation with T4-DNA-ligase the dsDNA was transformed into *E.coli* XL-Blue and the plasmids were analysed by *Bam*HI digestion.

From the resulting plasmid vector the 283 bp *Bam*HI fragment spanning the coding portion of exon 2 was excised and replaced by a 1.1 kbp *Bam*HI–*Bgl*II neomycin or a 2.2 kbp *Bam*HI hygromycin cassette in both orientations. A pilot electroporation with the four different constructs showed that the highest number of stably transformed ES cells was obtained with the neomycin construct inserted in opposite direction to the ND gene transcription direction (pNEOMNDG). The negative selection marker HSVtk was cloned as 1.8 kbp *Xba*I fragment 5′ to the *Eco*RI site of the homologous 6.5 kbp *Eco*RI fragment (Fig. 4a) within the *Xba*I site of the multiple cloning site of pNEOMNDG (see Fig. 4a), again in antiparallel orientation. Electroporation was carried out with the *Kpn*I linearized replacement vector, enabling the protection of the tk gene by 2.9 kbp pBluescript sequence. The neomycin, hygromycin as well as the tk cassette that were used have been described previously (22,31).

Gene targeting and tissue culture

Embryonic stem cells derived from mouse strain 129/Ola (line E14, kindly provided by A. Berns, Amsterdam) and feeder cells SNLH9 (22) were cultured in Dulbecco's modified Eagle's medium (DMEM) with 15 and 10% FCS, respectively, supplemented with 2 mM glutamine, 1 mM sodium pyruvate and 0.1 mM β-mercaptoethanol. For an initial pilot experiment, 5 µg linearized targeting construct were introduced by electroporation of 4 million ES cells in 800 µl supplemented DMEM with 15% FCS employing the Gene Pulser (Bio Rad, conditions: voltage 250 V, capacity 500 µF, pulse time 6–8 ms). Electroporated cells were resuspended in 20 ml supplemented DMEM + 15% FCS and plated in two 9 cm tissue culture dishes containing radiated SNLH9 feeder cells. Twenty-four h after plating selective medium was added, containing 350 µg/ml G418 or 300 µg/ml hygromycin B. Selective medium was refreshed every 2 days and after 10 days colonies became visible.

As the neo construct in opposite direction yielded highest efficiencies, this construct was used after introduction of the HSVtk gene for preparative electroporation. 20 µg linearized replacement vector DNA were electroporated into 20 million ES cells in 800 µl DMEM with 15% FCS. Electroporation and culturing was carried out as above, excepting the presence of 0.2 µM FIAU (1-[2-deoxy, 2-fluoro-β-D-arabinofuranosyl) additionally to G418 in the cell culture medium. After 10 days, 192 G418-resistant colonies were picked and transferred to 96-well plates. Colonies were expanded and splitted in two parts. One part was stored at –80°C in supplemented medium containing 10% DMSO. Of the other part DNA was isolated according to standard procedures, cleaved with *Bam*HI and resulting blots were hybridized with the 3′ probe, a 1.7 kbp

*Eco*RI–*Bam*HI fragment. Subsequently, the DNA of seven targeted ES cell lines was digested with *Bgl*II and analysed with the 5′ probe (1.8 kbp *Eco*RI fragment) and correct targeting was confirmed for six of them. Furthermore, metaphase spreads were analysed from each targeted cell line prior to injection. All of the six cell lines revealed the normal 40(X,Y) karyotype.

Generation and analysis of knock-out mice

Targeted clones were injected into 3.5 days blastocysts of C57Bl/6 mice and transferred into uterine horns of pseudopregnant foster mothers (C57Bl/6xCBA/Ca)F1 as described (32). Chimerism of resulting offspring was determined by coat colour, and males with more than 50% agouti coat colour were crossed with C57Bl/6 females. Resulting heterozygous F_1 females were bred with C57Bl/6 males. Germ-line transmission was scored and genotypes were analysed by PCR assay on tail biopsies. PCR was performed with 2 mND gene intron primers (forward: 5′ gtattgcatccatatttcttgg 3′, reverse: 5′ ctctccatcccctgacaagga 3′) in combination with two neo primers (neo5: 5 ggcctgggtggagaggcttttt 3′, neo3: 5′ ctatcgccttcttgacgagtt 3′). PCR amplifications were carried out in 10 mM Tris pH 8, 50 mM KCl, 6 mM $MgCl_2$, 5 mM DTT, 0.5 mM each dNTP, 250 µg/ml primer, 50–100 ng template and 0.8 units *Taq* DNA polymerase (Boehringer), for 35 cycles involving 1 min 94°C, 1 min 62°C and 1.5 min 72°C. The targeted locus will yield two fragments of 271 and 214 bp, and the wild-type locus results in a single 486 bp fragment. The progeny was again genotyped by PCR analysis of tail DNA.

Initial ophthalmological analysis was performed by direct slit-lamp biomicroscopy after dilatation of the pupils with 0.17% tropicamide. Prior to morphohistological analysis the eyes were enucleated and fixed for 2 h in Bouin solution. Serial sections of 5 µm were obtained from paraffin-embedded eyes and stained with hematoxylin and eosin according to standard histological protocols.

ACKNOWLEDGEMENTS

This research was supported by the Deutsche Forschungsgemeinschaft (DB, HH and WB).

REFERENCES

1. Warburg,M. (1961) Norrie's disease: A new hereditary bilateral pseudotumour of the retina. *Acta Ophthalmol.*, **39,** 757–772.
2. Warburg,M. (1966) Norrie's disease. A congenital progressive oculo–acoustico–cerebral degeneration. *Acta Ophthalmol.*, **89** (Suppl.), 1–147.
3. Warburg,M. (1975) Norrie's disease: Differential diagnosis and treatment. *Acta Ophthalmol.*, **53,** 217–236.
4. Nance,W.E., Hara,S., Hansen,A., Elliott,J., Lewis,M. and Chown,B. (1969) Genetic linkage studies in a Negro kindred with Norrie's disease. *Am. J. Hum. Genet.*, **21,** 423–429.
5. Moreira–Filho,C.A. and Neustein,I. (1979) A presumptive new variant of Norrie's disease. *J. Med. Genet.*, **16,** 125–128.
6. Hafez,M., El–Tahhan,H., Abdalla,A., Ibrahim,Z., Tawfik,A. and El–Desoky,M. (1982) A presumptive new presentation of Norrie's disease. *Egypt. J. Genet. Cytol.*, **11,** 213–225.
7. Gal,A., Wieringa,B., Smeets,D.F.C.M., Bleeker–Wagemakers,L. and Ropers,H.H. (1986) Submicroscopic interstitial deletion of the X chromosome explains a complex genetic syndrome dominated by Norrie disease. *Cytogenet. Cell Genet.*, **42,** 219–224.
8. Zhu,D., Antonarakis,S.E., Schmeckpeper,B.J., Diergaarde,P.J., Greb,A.E. and Maumenee,I.H. (1989) Microdeletion in the X–chromosome and prenatal diagnosis in a family with Norrie disease. *Am. J. Med. Genet.*, **33,** 485–488.
9. Donnai,D., Mountford,R.C. and Read,A.P. (1988) Norrie disease resulting from a gene deletion: clinical features and DNA studies. *J. Med. Genet.*, **25,** 73–78.
10. Gal,A., Bleeker–Wagemakers,L., Wienker,T.F., Warburg,M. and Ropers,H.H. (1985) Localization of the gene for Norrie disease by linkage to the DXS7 locus.(Abstract). *Cytogenet. Cell Genet.*, **40,** 633.
11. de la Chapelle,A., Sankila,E–M., Lindlöf,M., Aula,P. and Norio,R. (1985) Norrie disease caused by a gene deletion allowing carrier detection and prenatal diagnosis. *Clin. Genet.*, **28,** 317–320.
12. Berger,W., Meindl,A., van de Pol,T.J.R., Cremers,F.P.M., Ropers,H.H., Dörner,C., Monaco,A., Bergen,A.A.B., Lebo,R., Warburg,M., Zergollern,L., Lorenz,B., Gal,A., Bleeker–Wagemakers,E.M. and Meitinger,T. (1992) Isolation of a candidate gene for Norrie disease by positional cloning. *Nature Genet.*, **1,** 199–203.
13. Chen,Z-Y., Hendriks,R.W., Jobling,M.A., Powell,J.F., Breakefield,X.O., Sims,K.B. and Craig,I.W. (1992) Isolation and characterization of a candidate gene for Norrie disease. *Nature Genet.*, **1,** 204–208.
14. Sims,K.B., Lebo,R.V., Benson,G., Shalish,C., Schuback,D., Chen,Z–Y., Bruns,G., Craig,I.W., Golbus,M.S. and Breakefield,X.O. (1992) The Norrie disease gene maps to a 150 kbp region on chromosome Xp11.3. *Hum. Mol. Genet.*, **1,** 83–89.
15. Berger,W., van de Pol,D., Warburg,M., Gal,A., Bleeker–Wagemakers,L., de Silva,H., Meindl,A., Meitinger,T., Cremers,F. and Ropers,H.H. (1992) Mutations in the candidate gene for Norrie disease. *Hum. Mol. Genet.*, **1,** 461–465.
16. Fuentes,J–J., Volpini,V., Fernández–Toral,F., Coto,E. and Estivill,X. (1993) Identification of two new missense mutations (K58N and R121Q) in the Norrie disease (ND) gene in two Spanish families. *Hum. Mol. Genet.*, **2,** 1953–1955.
17. Wong,F., Goldberg,M.F. and Hao,Y. (1993) Identification of a nonsense mutation at codon 128 of the Norrie's disease gene in a male infant. *Arch. Ophthalmol.*, **111,** 1553–1557.
18. Fuchs,S., Xu,S.Y., Caballero,M., Salcedo,M., La O.A., Wedemann,H. and Gal,A. (1994) A missense point mutation (Leu13Arg) of the Norrie disease gene in a large Cuban kindred with Norrie disease. *Hum. Mol. Genet.*, **3,** 655–656.
19. Chen,Z–Y., Battinelli,E.M., Fielder,A., Bundey,S., Sims,K., Breakfield,X.O. and Craig,I.W. (1993) A mutation in the Norrie disease gene (NDP) associated with X–linked familial exudative vitreoretinopathy. *Nature Genet.*, **5,** 180–183.
20. Meindl,A., Berger,W., Meitinger,T., van de Pol,D., Achatz,H., Dörner,C., Haasemann,M., Hellebrand,H., Gal,A., Cremers,F. and Ropers,H.H. (1992) Norrie disease is caused by mutations in an extracellular protein resembling C–terminal globular domain of mucins. *Nature Genet.*, **2,** 139–143.
21. Meitinger,T., Meindl,A., Bork,P., Rost,B., Sander,C., Haasemann,M. and Murken,J. (1993) Molecular modelling of the Norrie disease protein predicts a cystine knot growth factor tertiary structure. *Nature Genet.*, **5,** 376–380.
22. van Deursen,J. and Wieringa,B. (1992) Targeting of the creatine kinase M gene in embryonic stem cells using isogenic and nonisogenic vectors. *Nucleic Acids Res.*, **20,** 3815–3820.
23. Warburg,M. (1968) Norrie's disease. *J. Ment. Def. Res.*, **12,** 247–251.
24. Parsons,M.A., Curtis,D., Blank,C.E., Hughes,H.N. and McCartney,C.E. (1992) The ocular pathology of Norrie disease in a fetus of 11 weeks gestational age. *Graefe's Arch. Clin. Exp. Ophthalmol.*, **230,** 248–251.
25. McDonald,N.Q. and Hendrickson,W.A. (1993) A structural superfamily of growth factors containing a cystine knot motif. *Cell*, **73,** 421–424.
26. Furukawa,Y., Uenoyama,S., Ohta,M., Tsunoda,A., Griffin,J.D. and Saito,M. (1992) Transforming growth factor β inhibits phosphorylation of the retinoblastoma susceptibility gene product in human monocytic leukemia cell line JOSK–I. *J. Biol. Chem.*, **267,** 17121–17127.
27. Ritzenhaler,J.D., Goldstein,R.H., Fine,A., Lichter,A., Rowe,D.W. and Smith,B.D. (1991) Transforming–growth–factor–β activation elements in the distal promoter regions of the rat alpha 1 type collagen gene. *Biochem. J.*, **280,** 157–162.
28. Chirgwin,J.M., Przybyla,A.E., MacDonald,R.J. and Rutter,W.J. (1979) Isolation of biologically active ribonucleic acid from sources enriched in ribonuclease. *Biochemistry*, **18,** 5294–5299.
29. Sambrook, J., Fritsch, E.F. and Maniatis, T. (1989) *Molecular cloning. A laboratory manual.* Cold Spring Harbor Laboratory Press, Cold Spring Harbor,
30. Bächner,D., Manca,A., Steinbach,P., Wöhrle,D., Just,W., Vogel,W., Hameister,H. and Poustka,A. (1993) Enhanced expression of the murine FMR1 gene during germ cell proliferation suggests a special function in both the male and female gonad. *Hum. Mol. Genet.*, **2,** 2043–2050.
31. van Deursen,J., Lovell–Badge,R., Oerlemans,F., Schepens,J. and Wieringa,B. (1991) Modulation of gene activity by consecutive gene targeting of one creatine kinase M allele in mouse embryonic stem cells. *Nucleic Acids Res.*, **19,** 2637–2643.
32. Bradley, A. Production and analysis of chimeric mice. In: *Teratocarcinomas and embryonic stem cells: a practical approach*, edited by Robertson, E.J. Oxford: IRL Press, 1987, pp. 113–151.